Structural Analysis of Historical Constructions – Jerzy Jasieńko (ed)
© 2012 DWE, Wrocław, Poland, ISSN 0860-2395, ISBN 978-83-7125-216-7

THREE-DIMENSIONAL EQUILIBRIUM ANALYSIS OF GOTHIC MASONRY VAULTS

Philippe Block[1], *Lorenz Lachauer*[2]

ABSTRACT

This paper introduces a powerful three-dimensional, computational equilibrium analysis method for masonry vaults using funicular networks. Applications of this new approach, based on Thrust Network Analysis and extended with insights from structural matrix analysis, for efficient funicular analysis of complex vault geometries are provided. This method provides the foundation for a fully three-dimensional limit analysis method for historic masonry vaults with complex geometries. The main concept and algorithms are introduced, and trough two exemplary case studies, the potential of this novel research is demonstrated. These discuss different assumptions on the flow of forces in Gothic quadripartite vaults, adding to the long historical debate on this topic, and provide a stability analysis of the intricate nave vaults of Sherborne Abbey, England.

Keywords: *Unreinforced masonry, Gothic vaults, Equilibrium analysis, Lower-bound analysis, Funicular analysis, Thrust Network Analysis*

1. INTRODUCTION

1.1. Limit analysis of masonry structures

Unreinforced masonry constructions generally fail not due to lack of compressive strength, but due to instability [1,2]. Understanding the equilibrium of structures in masonry is thus of primary concern. The importance of equilibrium methods for the analysis of masonry structure, framed in an extensive historical overview, is provided and argued very clearly by Huerta [3-5]. In order to determine the stability, and hence to assess the safety of masonry structures, a powerful structural theory based on limit analysis has been introduced by Heyman [6]. Within this framework, the *safe theorem* states that, under certain assumptions such as "enough" friction at the interfaces, it is sufficient to find a possible compression-only equilibrium state for the structure under the applied loads. In 2D, such equilibrium can be found, and visualized, by constructing a *thrust line* that fits within the geometry of the structure. Thrust line analysis is very powerful to explain the stability of two-dimensional structures, but unfortunately limited to them, although it can be used to perform conservative pseudo-3D analyses [7-10]. Boothby [11] provided a critical overview of the different analysis methods for masonry arches and vaults, and calls for the development of an automated three-dimensional version of graphical equilibrium analysis; a call which was echoed by Kurrer [12] and Marti [13].

1.2. Three-dimensional funicular analysis of masonry vaults

In order to extend thrust line analysis to fully 3D problems, O'Dwyer [14] introduced the use of three-dimensional funicular force networks that are fixed in plan. Using optimization, the nodal heights of compression-only networks that fit within the geometry of the structure could be generated. O'Dwyer's seminal work showed the importance of the topology of networks on the resulting equilibrium solutions and introduced different objectives. His approach was limited to simple examples (e.g. with high degrees of symmetry) as his framework did not include a general approach on how to deal with the static indeterminacies in the horizontal equilibrium of networks.

[1] PhD, Assistant Professor, Inst. of Technology in Architecture, ETH Zurich, Switzerland, pblock@ethz.ch
[2] Research Assistant, Inst. of Technology in Architecture, ETH Zurich, Switzerland, lalorenz@ethz.ch

Based on O'Dwyer's approach, Thrust Network Analysis (TNA) addressed this issue by introducing reciprocal force diagrams [15] that explicitly describe the possible horizontal equilibria of funicular networks under vertical loading [16-18]. TNA furthermore provided a general framework for linearizing O'Dwyer's equations of equilibrium for any type or topology of network. The original TNA framework still had an important drawback for the analysis of vaulted structures with complex geometries though: there was no general approach on how to automatically identify and control the degrees of freedom of the allowed reciprocal force diagrams for given force patterns, which are thus implicitly also the degrees of static indeterminacy of 3D funicular networks. The primarily "manual" manipulation of reciprocal diagrams is of course not sufficient to find equilibrium solutions for intricate, and thus highly dependent and statically indeterminate networks that fit within masonry vaulted structures with tight and complex geometries.
Other recent computational approaches for three-dimensional limit analysis using funicular networks can be found in Fraternali [19, 20], which Block [18] showed to be an equivalent framework to TNA, and Andreu et al. [21, 22].

2. LIMIT ANALYSIS FOR MASONRY

2.1. Introduction

Applying limit analysis using a thrust line or its three-dimensional, discretized extension, a *thrust network*, allows to formulate the hard problem of explaining the stability of a complex (vaulted) masonry structure as (primarily) a geometrical problem [25]. Although it is sufficient, based on the safe theorem, to find a possible equilibrium state for the vault, or in geometrical terms, a possible compression-only network that equilibrates the loading and stays within the vault's geometry, it is useful to identify specific equilibrium solutions, that allow one to make an assessment of the safety of the vaulted structure. Possible useful solutions are associated to the following objectives:

- Geometric safety factor (Fig. 1a), which is defined as the ratio between the thinnest possible arch/vault geometry enveloping a funicular solution in equilibrium with given loads over the actual vault geometry [26, 10], giving a measure of the vault's susceptibility under live loads.
- Minimizing/maximizing horizontal thrust (Fig. 1b), which provides the thrust values that bound the range of thrust that the arch/vault will and can exert onto its neighbouring elements (supports).
- Collapse load factor (Fig. 1c), which indicates how much live load an arch/vault can take before a collapse mechanism is formed, i.e. the thrust line no longer fits inside of the arch.

In 2D, there is furthermore a direct relation between the thrust lines in Figures 1b-1c and the collapse mechanisms: where the line touches the intrados and extrados on alternate sides, hinges will form [1].

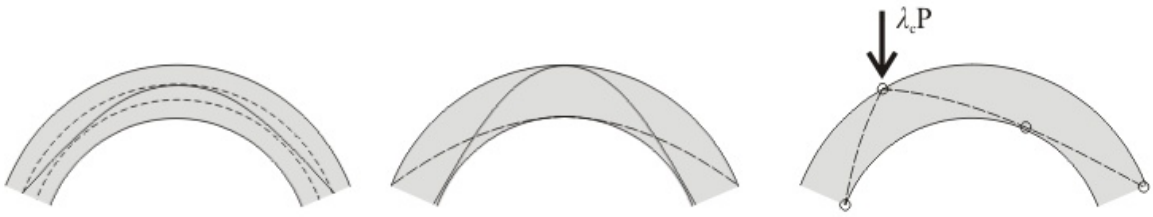

Fig. 1 Different relevant specific funicular solutions for an arch, providing a) the geometric safety factor; b) the minimum and maximum thrust; and c) the collapse load factor for a given live load location

2.2. Equilibrium of funicular networks

For the static analysis of (historic) masonry, which typically has a heavy, dominant self-weight, it is sufficient to consider vertical loading only. The vertical equilibrium of a typical node *i* in a funicular network (Fig. 2) is given by

$$F_{V,ji} + F_{V,ki} + F_{V,li} = P_i \tag{1}$$

in which $F_{V,ji}$ are the vertical components of forces in branches *ji*, and P_i is the load applied at node *i*.

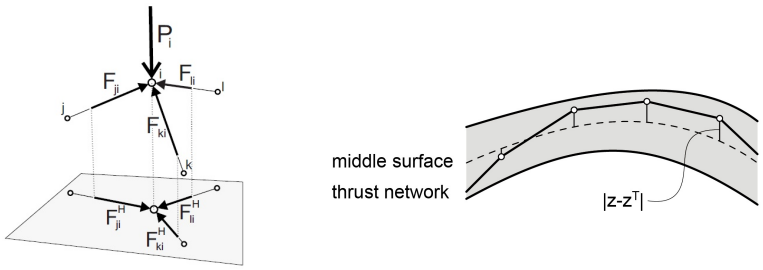

(a) (b)

Fig. 2 a) A typical node i in the funicular network with applied load P_i and branch forces F_{ji}, and b) the height deviation $|z\text{-}z^T|$ of the thrust network from the middle surface of the vault

For gravity loading, the lines of action of the loads are vertical, and it is thus meaningful to keep the horizontal projection of the laid-out network fixed during the analysis process. This is equivalent in 2D to thrust line analysis done using *graphic statics*, where indeed the nodes in the funicular form stay on the verticals through the centroids of single stones, called *voussoirs*, of a masonry arch [10]. Live loads are also applied at a specific (x,y)-location, and thus want to stay fixed during the analysis.
When rewriting the equilibrium equations in (1) in function of the horizontal force components, i.e. the thrusts in branches, $F_{H,ji}$, one gets:

$$\left(\frac{F_{H,ji}}{l_{H,ji}}+\frac{F_{H,ki}}{l_{H,ki}}+\frac{F_{H,li}}{l_{H,li}}\right)z_i-\frac{F_{H,ji}}{l_{H,ji}}z_j-\frac{F_{H,ki}}{l_{H,ki}}z_k-\frac{F_{H,li}}{l_{H,li}}z_l=P_i \tag{2}$$

in which $l_{H,ji}$ are the horizontal lengths of branches ji. This is the problem that O'Dwyer solves in [14], linearizing the equations by providing values for $F_{H,ji}$ after inspection of the network topology.
These $F_{H,ji}$ need to be chosen such that they represent a possible horizontal equilibrium. In TNA, this was guaranteed by constructing allowed compression reciprocal force diagrams, which then also allowed to linearize equations (2) by measuring the lengths of the corresponding reciprocal branches, $l^*_{H,ji}$, corresponding to these thrusts $F_{H,ji}$:

$$q_{ji}=\frac{F_{H,ji}}{l_{H,ji}}=\frac{l^*_{H,ji}}{l_{H,ji}} \tag{3}$$

with q_{ji} the well-known *force densities* [27] or *tension coefficients* [28].

2.3. Controlling the indeterminacy of funicular networks

For three-dimensional networks, obtaining one of the specific equilibrium solutions in Section 2.1 is not a straightforward task, because of the high degree of static indeterminacy of such models. Put simply, rather than having one horizontal thrust to consider, as for planar structures, these networks have highly dependent combinations of horizontal thrusts in their elements. This was clarified and visualized in TNA through the use of reciprocal force diagrams, which represent the different possible horizontal equilibria of these networks [16].
A strategy is needed to

1) identify a set of thrusts, or equivalently branch force densities, that can be chosen freely, independently from the others, and how the thrust values of the other, dependent branches then can be computed from these; and
2) control theses independent thrusts, the variables of the problem, in order to obtain one of the specific equilibrium solutions in Figure 1.

3. COMPUTATIONAL APPROACH

This section will outline the key steps of the new, nonlinear extension of TNA, which uses the matrix formulation of the Force Density Method [27] and enhances it with insights provided by matrix analysis of structural frames [28]. For a detailed description of the mathematical formulations and algorithms involved and implemented, the authors refer to [24, 29].

3.1. Overview problem

Addressing the first question in Section 2.3, Block and Van Mele [29] introduced a new approach for identifying the force dependencies between branches in equilibrium networks with parallel loads and fixed projection, based on matrix analysis of structural frames [28,30]. The main concept is that, because only vertical loads are considered, each in-plane equilibrium of the (unloaded) 2D bar-node structure, which coincides with the projection on the plane of the funicular network, represents a possible horizontal equilibrium of a funicular network for the given loads. These equilibria correspond to the *states of self-stress* of that planar structure, and identifying these, then give the *independent branches* of the network, i.e. the branches whose thrusts, or equivalently force densities $\mathbf{q}_{\text{indep}}$, can be chosen freely without violating the equilibrium of the fixed planar network topology.

Concerning the second question in Section 2.3, this paper will focus on one of the objectives: finding the geometric safety factor (Fig. 1.a), which can be equivalently formulated as a function of the solution which minimizes the least-squared "closest-fit" solution to the mid surface of the vault (Fig. 2a):

$$f(\mathbf{q}_{\text{indep}}) = \left\| \mathbf{z} - \mathbf{z}^{\text{M}} \right\|_2 \tag{4}$$

with $\mathbf{z}^{\text{M}} = (\mathbf{z}^{\text{I}} + \mathbf{z}^{\text{E}})/2$, $\mathbf{z}^{\text{I}}$ and $\mathbf{z}^{\text{E}}$ being the intrados and extrados heights of the vault. Additionally, one needs to enforce that all $\mathbf{q}$ are positive to guarantee a compression-only solution.

3.2. Solving procedure

Finding the closest-fit solution for a funicular network with fixed projection can, as mentioned above, be reduced to finding the set of $\mathbf{q}_{\text{indep}}$ that minimizes the global objective (4). As these variables do not explicitly appear in the objective function, this problem is solved using a *black-box* function which allows to describe the convoluted objection function $f(\mathbf{z}(\mathbf{q}(\mathbf{q}_{\text{indep}})))$ implicitly in several steps:

$$\mathbf{q}_{\text{indep}} \rightarrow \mathbf{q} \rightarrow \mathbf{z} \rightarrow f(\mathbf{z}) \tag{5}$$

where the first two are linear transformations, and the last step involves taking the least-squares. These steps that need to be computed at each iteration, can be solved fast.

Even though the closest-fit constrained optimization problem is non-linear and non-convex, it can be solved efficiently with the computationally inexpensive implicit black-box function (5), by using a quasi-Newton search method, and by providing the gradient vector of the objective function f, which can be computed using the chain rule [27,23]. It is important to use good starting points for the search because of the non-convexity of the problem. These want to be informed by the network topology and target surface [24].

Lastly, it is important to note that finding this closest-fit solution forms the basis for finding the two other objectives discussed in Section 2.1, as it provides a good, feasible starting point for these two other objectives.

4. APPLICATIONS

4.1. Flow of forces in a quadripartite vault

Viollet-le-Duc's assumptions [31] on how forces run in masonry vaults were corrected by Abraham [32], explaining that the "real" direction of the forces were as the trajectories of a cannon ball dropped on the extrados vault when rolling to the supports. Ungewitter and Mohrmann [8] and Rave [33] defined the force paths in masonry vaults by cutting them up according to lines of steepest descent; Heyman [34, 35] explained that gothic vaults acted as thin shells with stress concentrations along creases; Mark et al. [36] found the "exact" flow of forces in gothic vaults based on the results of photo-elastic analysis on plexi-glass scale models; Barthel [37] studied gothic vaults using non-linear FEM analysis, but also provided a clear discussion of this topic looking at several vault geometries and relating it to typically observed crack patterns; and O'Dwyer [14] proposed that a good discretization should combine, or at least reflect, all possible ways the forces in the vault could act.

It is clear that there has been a long-lasting discussion on how gothic vaults exactly work. This section shows that with the approach presented in this paper a systematic comparison between these different assumptions is now possible. Thanks to the new algorithms, the different assumptions on the force

paths can be evaluated and discussed using quantifiable measures, by e.g. comparing for each one of them the obtained geometric safety factor.
Figure 3 shows the generic quadripartite vault geometry which we used as example, constructed following Fitchen's geometrical diagrams [38].

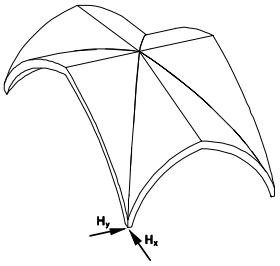

Fig. 3 Generic quadripartite vault geometry with dimensions 13 m × 7 m × 4.5 m, and horizontal thrust at the corners in both x- and y-direction

As discussed before, each assumption on the force flow can be abstracted to a discrete network, constructed in plan. Figures 4-6 show the results of four different layouts of force networks. The first pattern (a) assumes parallel arches carried to the supports by rib arches; the second (b) assumes arches, arranged in a fan-like form, going directly to the supports; the third (c) is a superposition of the first two patterns; and the last pattern (d) combines a regular quadrilateral grid with arches in plan going to the supports, a free interpretation of Mark's assumptions. The patterns are laid out such that they only have a thrust components at the corners. For each network topology, the least-squares closest-fit solution to the centre surface of the vault geometry is compared for this generic quadripartite vault, considering the self-weight of the vault only, without fill.

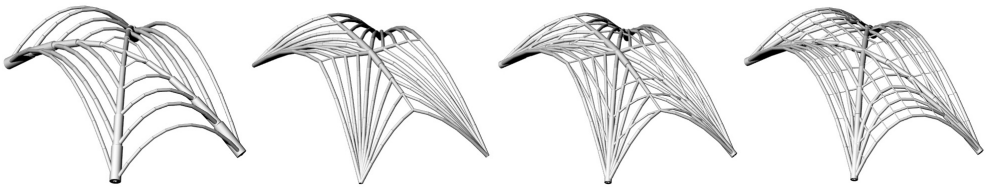

Fig. 4 Resulting closest-fit solutions to the target surface, chosen as the mid surface of the vault geometry in Figure 3; the pipes around the branches of the funicular network visualize the magnitude of force in them

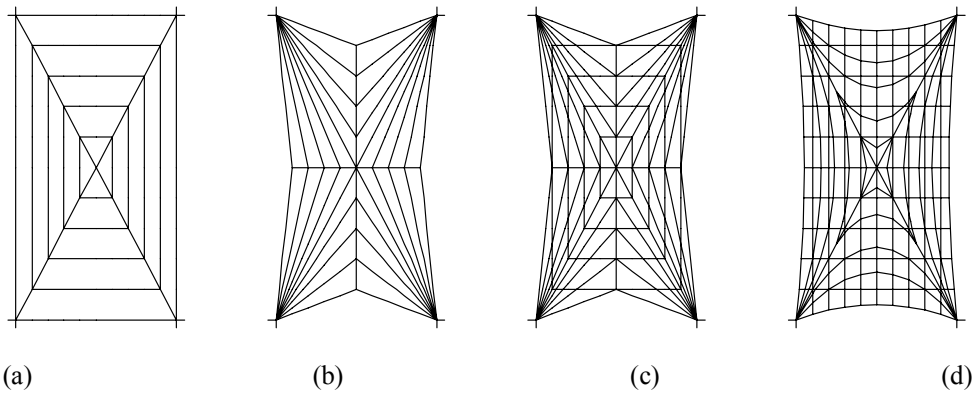

Fig. 5 Four different force patterns: a) parallel arches and rib arches; b) a fan-like arrangement of arches directly going to the corner supports; c) a superposition of the first two patterns; and d) a pattern which combines a regular quadrilateral grid with arches in plan going to the supports

Table 1 shows the summary of the results obtained with the closest-fit solving algorithm for the different force patterns in Fig. 4-6, with m, the number of branches; n_i, the number of free nodes; the number of iterations; the objective function $f(z) = ||z\text{-}z^M||_2$, divided by the number of free nodes; the maximum and average vertical deviation $|z\text{-}z^M|$ (absolute value) of the compression solution z and the target surface z^M; and, t, the solving time in seconds (using a MacBook Pro with an Intel DuoCore processor, 2.8 GHz).

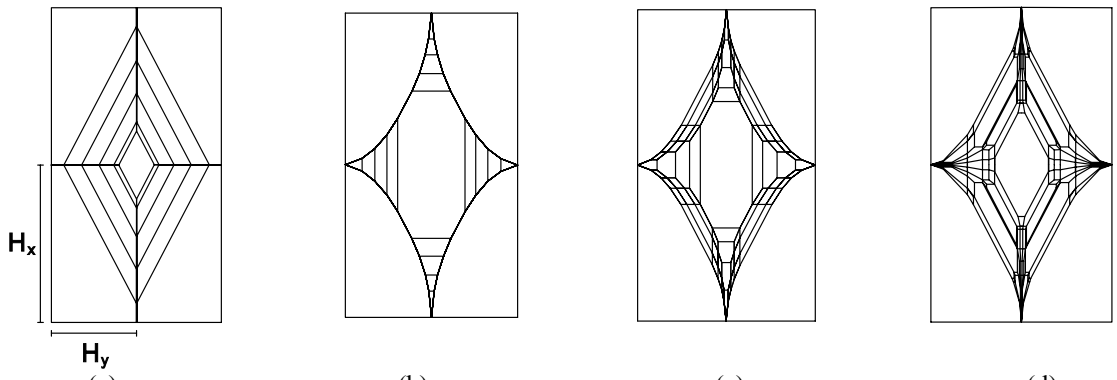

Fig. 6 The reciprocal force diagrams, corresponding to the respective closest-fit solutions for the four patterns in Figure 5 and drawn to the same scale, show the distribution of thrusts. Although the horizontal thrust in x- and y direction at the corner supports differ less than 5%, the thrusts are redistributed very differently inside of the vault for each solution

Table 1 Results of the closest-fit solving for the different force patterns in Figs. 4-6: m, the number of branches; n_i, the number of free nodes; the number of iterations; the least-squares objective function $f(z) = \|z\text{-}z^M\|_2$, divided by the number of free nodes; the maximum and average vertical deviation $|z\text{-}z^M|$ (absolute value) of the compression solution z and the target surface z^M; and, t, the solving time in seconds.

Pattern	m	n_i	k	iter	f / n_i [mm^2]	$\|z\text{-}z^M\|_{max}$ [mm]	$\|z\text{-}z^M\|_{aver}$ [mm]	**t** [sec]
a	148	121	10	55	1778	142	29	0.839
b	252	213	18	95	242	54	12	1.976
c	380	261	34	249	**187**	62	13	7.027
d	480	225	36	526	337	84	10	17.423

It is not surprising that pattern (a) performs worst, as the simple arches running across the web of the vault will have approximately catenary shapes and will thus never fit a pointed vault well. A remarkable improvement is observed for pattern (b). Indeed, this fan-like arrangement is connected at the vault's ridges allowing for a "kink" in the funicular arches which are going across the web. The best solution is achieved with the superposed pattern (c). Notice though that the improvement over (b) is not that significant, which can be explained/seen by comparing their reciprocal diagrams: indeed the reciprocal diagram of pattern (c) globally has similar thrust distributions as the one for pattern (b). Pattern (d) does not perform better as the topology of the network is pretty constraining along the non-supported boundaries, due to the deterministic three-valent nodes (cf. Section 2.3).
These findings add a new contribution to the historic discussion, and provide new arguments and insights to come closer to a full understanding of the structural behaviour of masonry vaults. A more extensive comparative study using this approach might provide a possible synthesis of the different assumptions on the force paths. Such an exploration would only have value though for specific, built vaults. It is important though to remember that all of these solutions are just lower-bound solutions, which do not represent the "real" state of the vault; this one, we will never know.

4.2. Complex Gothic vault geometry

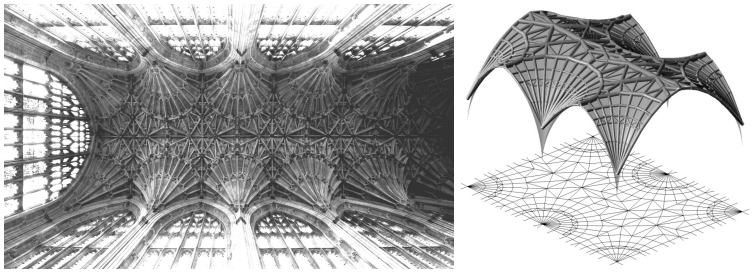

Fig. 7 Nave Vault of the Sherborne Abbey, Dorset, UK (Photo by Lawrence Lew, lawrence.lew@english.op.org/); and target surface and piped closest-fit solution

This section looks at the equilibrium of the nave vaults of Sherborne Abbey in Dorset, England, finished around 1490 (Fig. 7). These intricate vaults are a cross between lierne and fan vaults. From plans and section, complemented with photographs, a simplified 3D model was made of the vaults. The main features of the vault then served as guide to draw a force pattern (Fig. 8a).
The pattern in Figure 8.a has 949 branches and 462 nodes. The problem is reduces to 183 variables, showing that this is a highly statically indeterminate problem. The closest-fit funicular network was solved in less than 8 min, showing that intricate network topologies, and complex vault geometries, can be solved efficiently, and that the solving algorithm is robust, even for large problems.

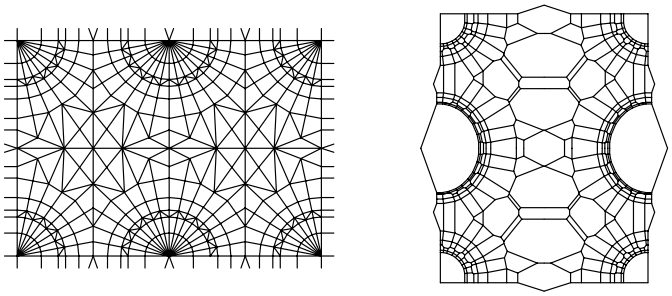

(a) (b)

Fig. 8 (a) Form diagram, directly using the rib layout of the vaults, and (b) the resulting closest-fit reciprocal force diagram

5. CONCLUSION

This paper showed through examples a robust and efficient solving algorithm for finding closest-fit funicular network for masonry vaults with complex geometries. These solutions correspond to the geometric safety factor for these structures. The presented framework, which extended Thrust Network Analysis using matrix analysis, can be seen as a strong foundation for fully three-dimensional equilibrium analysis of vaulted masonry.
Future work will include new optimization formulations that use this closest-fit solution to e.g. obtain the minimum and maximum thrust solutions of vaults or compute the collapse load factor for critical live loading cases. It is important to fully control all the degrees of indeterminacy in order to obtain such an absolute minimum or maximum thrust solution. The hope is that, as in two-dimensional arch analysis, these thrust networks can provide information about possible collapse mechanisms for fully three-dimensional problems. These results can then be compared with other approaches for stability assessment of masonry structures such as presented in [39].

REFERENCES

[1] Heyman J. (1995) *The Stone Skeleton: Structural engineering of masonry architecture.* Cambridge University Press, Cambridge,
[2] Ochsendorf J.A. (2002) Collapse of masonry structures. PhD dissertation, University of Cambridge, Cambridge,
[3] Huerta S. (2001) Mechanics of Masonry Vaults: The equilibrium approach. In: *Proceedings of Historical Constructions,* Guimaeres, 47-69,
[4] Huerta S. (2004) *Arcos bóvedas y cúpulas. Geometría y equilibrio en el cálculo tradicional de estructuras de fábrica.* Instituto Juan de Herrera, Madrid,
[5] Huerta S. (2008) The Analysis of Masonry Architecture: A Historical Approach. *Architectural Science Review* 51(4): 297-328,
[6] Heyman J. (1966) The stone skeleton. *International Journal of Solids and Structures* 2: 249-279,
[7] Wittmann W. (1879) Zur Theorie der Gewölbe. *Zeitschrift für Bauwesen* 26: 61-74,
[8] Ungewitter G. (1890) *Lehrbuch der gotischen Konstruktionen* (IIIrd Ed., Reworked by K. Mohrmann). T.O. Weigel Nachfolger, Leipzig,
[9] Wolfe W.S. (1921) *Graphical Analysis: A handbook on graphic statics*. McGraw-Hill Book Company, New York.
[10] Block P., Ciblac T., Ochsendorf J.A. (2006) Real-time limit analysis of vaulted masonry buildings. *Computers & Structures* 84(29-30): 1841-1852.

[11] Boothby T.E. (2001) Analysis of masonry arches and vaults. Progress in Structural Engineering and Materials 3(3): 246-256.
[12] Kurrer K.-E. (2008) *The History of the Theory of Structures. From Arch Analysis to Computational Mechanics*. Ernst & Sohn, Berlin.
[13] Marti P. (2012) *Baustatik: Grundlagen, Stabtragwerke, Flächentragwerke*. Ernst & Sohn, Berlin.
[14] O'Dwyer D. W. (1999) Funicular analysis of masonry vaults. *Computers & Structures* 73(1-5): 187-197.
[15] Maxwell J.C. (1864) On reciprocal figures and diagrams of forces. *Philosophical Magazine and Journal Series* 4(27): 250-261.
[16] Block P., Ochsendorf J. (2007) Thrust Network Analysis: A new methodology for three-dimensional equilibrium. *Journal of the International Association for Shell and Spatial Structures* 48(3): 167-173.
[17] Block P., Ochsendorf J. (2008) Lower-bound analysis of masonry vaults. In: *Proceedings of the 6th International Conference on Structural Analysis of Historic Construction*, Bath, UK.
[18] Block P. (2009) Thrust Network Analysis: Exploring Three-dimensional Equilibrium. PhD dissertation, Massachusetts Institute of Technology, Cambridge.
[19] Fraternali F., Rocchetta G. (2002) Shape optimization of masonry vaults. In: *Proc. of the 2nd International Conference on Advances in Structural Engineering and Mechanics*, Busan, Korea.
[20] Fraternali F. (2010) A thrust network approach to the equilibrium problem of unreinforced masonry vaults via polyhedral stress functions. *Mechanics Research Communications* 37: 198-204.
[21] Andreu A., Gil L., Roca P. (2007) Computational analysis of masonry structures with a funicular model. *Journal of Engineering Mechanics* 133(4): 473-480.
[22] Andreu A., Gil L., Roca P. (2010) Analysis of masonry structures by funicular networks. Proceedings of the ICE – Engineering and Computational Mechanics 163(3): 147-154.
[23] Block P., Lachauer L. (2011) Closest-Fit, Compression-Only Solutions for Free-Form Shells. In: *Proceedings of the IABSE-IASS Symposium*, London, UK.
[24] Block P., Lachauer L. (2012) Advanced Funicular Analysis of Masonry Vaults. *Computers & Structures*, submitted for review.
[25] Van Mele T., Rippmann M., Lachauer L., Block P. (2012) Geometry-based Understanding of Structures. *Journal of the International Association of Shell and Spatial Structures* 53(2).
[26] Heyman, J. (1982) *The Masonry A*rch. Ellis Horwood, Chichester.
[27] Schek H.-J. (1974) The force density method for formfinding and computation of general networks. *Computer Methods in Applied Mechanics and Engineering* 3(1): 115-134.
[28] Pellegrino S., Calladine C.R. (1986) Matrix analysis of statically and kinematically indeterminate frameworks. *International Journal of Solids and Structures* 22(4): 409-428.
[29] Block P., Van Mele T. (2012) Algebraic Graphical Analysis. *International Journal of Solids and Structures*, submitted for review.
[30] Pellegrino S. (1993) Structural Computations with the Singular Value Decomposition of the Equilibrium Matrix. International Journal of Solids and Structures 30(21): 3025-3035.
[31] Viollet-le Duc E.E. (1854-1868) Dictionnaire raisonné de l'architecture française du XIe au XVIe siècle, Vol. 2 : «Construction». B. Bance, Paris.
[32] Abraham P. (1934) *Viollet-le-Duc et le Rationalisme Médiéval*. Fréal & Cie, Paris.
[33] Rave W. (1939) Über die Statik mittelalterlicher Gewölbe. *Deutsche Kunst- und Denkmalpflege* 1939/1940: 193-198.
[34] Heyman J. (1968) On the rubble vaults of the middle ages and other matters. *Gazette des Beaux-Arts* 71: 177-188.
[35] Heyman J. (1977) *Equilibrium of Shell Structures*. Oxford Engineering Science Series, Clarendon Press, Oxford.
[36] Mark R., Abel J.F., O'Neill K. (1973) Photoelastic and finite-element analysis of a quadripartite vault. *Experimental Mechanics* 13(8): 322-329.
[37] Barthel R. (1994) Tragverhalten gemauerter Kreuzgewölbe. In: *Aus Forschung und Lehre 34*. Institut für Tragkonstruktionen, Universität Karlsruhe, Karlsruhe.
[38] Fitchen J. (1961) *The Construction of Gothic Cathedrals – A study of Medieval vault erection*, University of Chicago Press, Chicago.
[39] Van Mele T., McInerney J., DeJong M.J., Block P. (2012) Physical and Computational Discrete Modelling of Masonry Vault Collapse. In: *Proc. of the 8th International Conference on Structural Analysis of Historic Construction*, Wroclaw, Poland.